COHERENT AND INCOHERENT OPERATION IN OPTICAL VIBRATION MICROSCOPY

A. Korpel and H. Snyder

Department of Electrical and Computer Engineering

The University of Iowa, Iowa City, IA 52242

Abstract

We present an experimental and theoretical analysis of vibration microscopy using an arbitrarily defined detection aperture. In the two limiting cases, incoherent operattion (no aperture) offers intensity gradient information in the amplitude of higher harmonics of the vibration frequency, while coherent operation (pinhole aperture) reflects the phase of the object being scanned in the amplitude of the first harmonic. The possibilities of phase microscopy, when using the system in a coherent mode of operation, are discussed. Vibrating knife edge, incoherent, coherent, phase microscopy

1. Introduction

In previous papers [1,2,3], we have described a sampling optical microscope with electronically variable resolution. In its one-dimensional mode of operation, the microscope utilizes an optically opaque vibrating knife edge (razor blade) placed in a laser beam, close to a partially transmissive amplitude object to be scanned. The transmitted, modulated light from the vicinity of the knife edge constitutes the useful signal, as it carries local information about the object. This information is extracted through photodetection and bandpass filtering and used to form a picture of the object.In [2]

it is shown that resolution of the device is on the order of the amplitude of vibration of the knife edge. An extension of the method to two dimensions involving tomography is discussed in [4].

The present paper reports on incoherent operation (all light detected excluding evanescent waves) and coherent operation (some light filtered out), and the possibility of phase microscopy in the latter.

The paper is organized as follows.Section 2 discusses what we have called partially coherent operation in which the detection aperture is an amplitude mask of arbitrary specification. We first derive the expression for the total photodetector current in this general case, and then investigate the limits of incoherent and coherent operation. The incoherent case is characterized by an infinite aperture and leads to detection of integrated intensities. In the fully coherent case the aperture is a pinhole, resulting in detection of the integrated amplitude of the field.

Following the analyses of these limiting cases, we derive, for partially coherent operation, the fundamental AC current component. The resulting expression is applied to a Gaussian slit (a model that makes explicit evaluation possible) and the results compared with a physical experiment employing a rectangular slit.

In Section 3 we examine in more detail the limiting cases of incoherent and coherent detection. For the incoherent case we take into account all higher harmonics of the fundamental frequency, and show that the amplitude of the nth harmonic is proportional to the (n-1)th partial derivatives of the intensity distribution at the knife edge. This is confirmed by a simple experiment.

For coherent operation, we limit ourselves for simplicity to the first harmonic, and show that this component carries information about the phase of the sampled region relative to the phase of the surrounding area. This is investigated in detail in Section 4, and exemplified by the application of our theory to the field distribution behind a lens. Experimental results are seen to back up the calculations.

Finally, in Section 5 we state conclusions and suggest future research.

2. Partially Coherent Operation

In this section the general expression for the current generated by a photodetector with an arbitrary aperture will first be derived, followed by the first harmonic component of the current in the case of a vibrating knife edge. Finally the first harmonic current found when employing a Gaussian aperture in the derived equations will be compared with an experiment using a variable slit in front of the photodetector.

For our model we assume that a quasi-monochromatic field $E_1(x,y,t)$ is mapped by a Fourier transforming lens with focal length F into a field $E_2(x_2,y_2,t)$ in the back focal plane. Using spatial frequency coordinates $f_x = x_2/F\lambda$, $f_y = y_2 / F\lambda$, (λ = light wavelength) we find from the Fourier transforming properties of the lens

$$E_2(f_x,f_y,t) \quad \int_{-\infty}^{\infty}\int_{-\infty}^{\infty} E_1(x,y,t)\exp(+j2\pi f_x x + j2\pi f_y y)\, dxdy \qquad (1)$$

where we use the Electrical Engineering convention for phasors.

After being apertured by an amplitude mask $G(f_x,f_y)$ in the back focal plane of the lens, the field is incident on a photodetector, generating a current

$$i(t) \quad \int_{-\infty}^{\infty}\int_{-\infty}^{\infty} |E_2(f_x,f_y,t)G(f_x,f_y)|^2 \, df_x df_y \tag{2}$$

According to Parseval's theorem [5] this may also be written as

$$i(t) \quad \int_{-\infty}^{\infty}\int_{-\infty}^{\infty} |F\{E_2(f_x,f_y,t)G(f_x,f_y)\}|^2 \, dxdy \tag{3}$$

where F denotes the Fourier transform. Using a well known property of the Fourier transform we may write for (3)

$$i(t) \quad \int_{-\infty}^{\infty}\int_{-\infty}^{\infty} |F\ \{E_2(f_x,f_y,t)\} * F\ \{G(f_x,f_y)\}|^2 \, dxdy \tag{4}$$

where the asterisk denotes convolution. Introducing the function

$$g(x,y) = F\ \{G(f_x,f_y)\} \tag{5}$$

and using eq. (4), we find finally:

$$i(t) \quad \int_{-\infty}^{\infty}\int_{-\infty}^{\infty} |E_1(x,y,t) * g(x,y)|^2 \, dxdy. \tag{6}$$

Eq. (6) is the basis equation to be used for calculating partially coherent detection subject to an arbitrary aperture G.

We now apply this general expression to the two limiting cases of incoherent and coherent detection.

Incoherent Case

In the incoherent case, we assume that all the light is detected, thus the aperture $G(f_x,f_y) = 1$. When the Fourier transform of the aperture $\{g(x,y) = \delta(x)\,\delta(y)\}$ is substituted into eq. (6), we have for the incoherent mode

$$i(t) \quad \int_{-\infty}^{\infty}\int_{-\infty}^{\infty} |E_1(x,y,t)|^2 \, dxdy. \tag{7}$$

Evidently in the incoherent case we detect the integrated intensity, as previously stated.

Coherent Case

In the coherent case, we utilize a pinhole detector to aperture the photodetector. For mathematical simplicity, we model the mask as:

$$G(f_x,f_y) = \lim_{B\to 0} \ \mathrm{sinc}(f_x/B)\ \mathrm{sinc}(f_y/B) \tag{8}$$

so that

$$g(x,y) = \lim_{B\to 0} \ B^2 \mathrm{rect}(xB)\ \mathrm{rect}(yB). \tag{9}$$

If it is assumed that E_1 is limited to an area $A^2 << (1/B)^2$ (always true if $B \to 0$ and A is finite) then it may be shown readily that

$$E_1(x,y,t)*g(x,y) \rightarrow B^2 \int_{-A/2}^{A/2}\int_{-A/2}^{A/2} E_1(x',y',t)\,dx'dy' \quad \text{for } |x|,|y| < 1/2B$$

$$\rightarrow 0 \quad \text{elsewhere.} \qquad (10)$$

We then find from eq. (6)

$$i(t) \qquad B^2 \left| \int_{-\infty}^{\infty}\int_{-\infty}^{\infty} E_1(x,y,t)\,dxdy \right|^2 \quad \text{for } B \rightarrow 0. \qquad (11)$$

Hence, as mentioned before, the coherent case involves an integration of the complex amplitude of the field. The implications of eq. (11) for phase microscopy will be discussed in Sec.4.

<u>First Harmonic</u>

We will now derive an expression for the first time harmonic component of the detector current for the case of weak modulation by a knife edge. We write the field $E_1(x,y,t)$ as follows

$$E_1(x,y,t) = U(x-x_o-\Delta\cdot\cos(\omega t))\cdot E_i(x,y) \qquad (12)$$

where the knife edge, nominally situated at x_o and vibrating as $\Delta\cdot\cos(\omega t)$, is represented by the step function $U(x-x_o-\Delta\cdot\cos(\omega t))$, and $E_i(x,y)$ denotes the illuminating field. For simplicity we write $\cos(\omega t) = u$ and set

$$E_1(x,y,t) \rightarrow E_1(x,y,u) = U(x-x_o-\Delta\cdot u)\cdot E_i(x,y). \qquad (13)$$

Hence eq. (6) then becomes

$$i(u) \qquad \int_{-\infty}^{\infty}\int_{-\infty}^{\infty} |E_i(x,y)\cdot U(x-x_o-\Delta\cdot u) * g(x,y)|^2\,dxdy$$

$$= \int_{-\infty}^{\infty}\int_{-\infty}^{\infty} [E_i(x,y)\cdot U(x-x_o-\Delta\cdot u) * g(x,y)] \times$$

$$[E_i^*(x,y)\cdot U(x-x_o-\Delta\cdot u) * g^*(x,y)]\, dxdy \qquad (14)$$

where * denotes the complex conjugate. We now expand the current i(u) in a Taylor series so that to a first order

$$i(u) = i(0) + i'(0)u \qquad (15)$$

where $i'(0) = \left.\frac{\partial i}{\partial u}\right|_0$. From eq. (14) it follows that

$$i'(0)$$

$$-\Delta \int_{-\infty}^{\infty}\int_{-\infty}^{\infty} \left(\int_{-\infty}^{\infty}\int_{-\infty}^{\infty} \delta(x''-x_o)E_1(x'',y'')g(x-x'',y-y'')dx''dy'' \times \right.$$

$$\left. \int_{-\infty}^{\infty}\int_{-\infty}^{\infty} E_1^*(x',y')U(x'-x_o)g^*(x-x',y-y')dx'dy' \right) dxdy + cc. \qquad (16)$$

where cc denotes the complex conjugate.

Using the sifting property of the delta function, this may be written as

$$i'(0) \quad -\Delta \int_{-\infty}^{\infty}\int_{-\infty}^{\infty} \left(\int_{-\infty}^{\infty} E_1(x_o,y'')g(x-x_o,y-y'')\, dy'' \times \right.$$

$$\left. \int_{-\infty}^{\infty}\int_{-\infty}^{\infty} E_1^*(x',y')U(x'-x_o)g^*(x-x',y-y')dx'dy' \right) dxdy + cc. \qquad (17)$$

We now first perform the integration I_a over x and y:

$$I_a = \int_{-\infty}^{\infty}\int_{-\infty}^{\infty} g(x-x_o,y-y'')g^*(x-x',y-y')\, dxdy. \qquad (18)$$

Substituting $v = x-x_o$, $w = y-y''$, we find readily that this may be written as

$$I_a = \int_{-\infty}^{\infty}\int_{-\infty}^{\infty} g(v,w)g^*[v-(x'-x_o),w-(y'-y'')]\, dxdy. \qquad (19)$$

Defining the (two-dimensional) autocorrelation function of g as

$$g_a(\xi,\psi) = \int_{-\infty}^{\infty}\int_{-\infty}^{\infty} g(v,w)g^*(v-\xi,w-\psi)\, dvdw. \qquad (20)$$

(17) may be written as

$$i'(0) \quad -\Delta \int_{-\infty}^{\infty}\int_{-\infty}^{\infty} \left[\int_{-\infty}^{\infty} E_1(x_o,y'')g_a(x'-x_o,y'-y'')dy''\right] x$$

$$E_1^*(x',y')U(x'-x_o)\, dx'dy' + cc. \qquad (21)$$

Gaussian Analysis

` In the following, eq.(21) for the first harmonic current will be applied to the case where a gaussian illuminating beam is used in conjunction with (for simplicity) a gaussian aperture.

` The gaussian illuminating field is described as

$$E_i(x,y) = A\exp(-x^2/w_o^2)\ \exp(-y^2/w_o^2) \qquad (22)$$

and the gaussian amplitude filter in the focal plane (at the photodetector) is given by

$$G(f_x,f_y) = \exp(-f_x^2/f_1^2)\ \exp(-f_y^2/f_2^2) \qquad (23)$$

where f_1 and f_2 are the mask dimensions. Substituting eqs (22) and (23) into (21), we find, after tedious calculus, that

$$i'(0) \quad -\Delta|A|^2 \sqrt{\frac{\pi}{2}}\, w_o \frac{(\pi w_o f_1/\sqrt{2})}{\sqrt{1+(\pi w_o f_1/\sqrt{2})^2}} \frac{(\pi w_o f_2)}{\sqrt{1+(\pi w_o f_2)^2}}. \qquad (24)$$

To shed some light on this equation, it has been graphed using *Maple V* and is shown in Figure 1 as a dashed line.

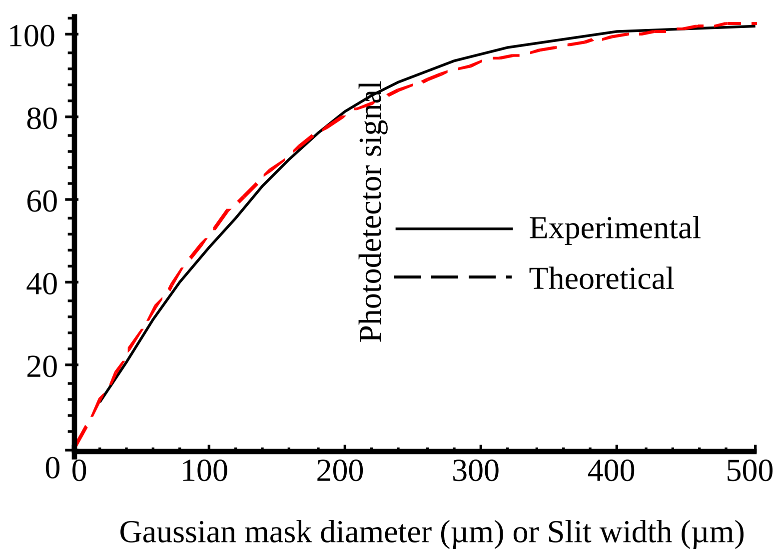

Fig. 1. First-harmonic Gaussian mask (theoretical) plotted versus a rectangular slit (experimental).

To check the predictive power of eq. (24) we performed a physical experiment as follows. A knife edge vibrating at a frequency of 284 Hz was placed in the center of a laser beam, and the modulated light then collected by a lens and focused onto a variable width rectangular slit (0 - 500 μm) in front of a photodetector. The beam diameter of the focused spot was about 230 μm. The first harmonic of the current was detected with a lock-in amplifier. Figure 1 depicts the experimental data plotted as a solid line. As would be expected, the first harmonic increases streadily and then starts leveling off when the slit is around 230 μm (same size as the focused beam) where incoherent operation is approached. The best fit between the two curves was obtained when the center to 1/e width of the Gaussian slit was chosen to equal 76 % of the actual physical width of the rectangular aperture.

2. Incoherent and Coherent Operation

Incoherent Operation

The incoherent mode of operation is characterized by an infinitely large photodetector *accepting all propagating waves that pass the knife edge*. (We do not consider evanescent waves in our analysis.) Our model consists of a vibrating knife edge and object positioned in the same plane in the beam, before the Fourier transforming lens. The position of the knife edge at any instance of time is again given by $x(t) = x_o + \Delta\cos(\omega t)$. The time varying current from the photodetector may be written from (7) and (12) as

$$i(t) \quad \int_{-\infty}^{\infty}\int_{x(t)}^{\infty} |E_i(x,y)|^2 dxdy \quad \int_{-\infty}^{\infty}\int_{x(t)}^{\infty} I_i(x,y)dxdy \qquad (25)$$

where $I_i(x,y) \quad |E_i(x,y)|^2$ denotes intensity. After separating (25) into its constant and harmonic currents, applying a change of variables and expanding into a Taylor series about x_o with Δ assumed small, we find:

$$i(t) \quad i_o + a_1\cdot\cos(\omega t) + a_2\cdot\cos(2\omega t) + a_3\cdot\cos(3\omega t)$$
$$+ a_4\cdot\cos(4\omega t) + a_5\cdot\cos(5\omega t) \qquad (26)$$

where

$$i_o = \int_{-\infty}^{\infty} \int_{x_o}^{\infty} I_1(x,y)dxdy \qquad (27)$$

and

$$a_n \quad \Delta^{n-1} \int_{-\infty}^{\infty} \left. \frac{\partial^{n-1} I_i(x,y)}{\partial x^{n-1}} \right|_{x_o} dy \quad \text{for } n = 1,2,3... \qquad (28)$$

where for all harmonics we have ignored powers of Δ higher than the first one encountered. It is interesting that expressions similar to (26) and (28) are found in ref [6] where the authors use a periodically deflected beam to scan an object.

Eqs (26) and (28) were checked by the following experiment. A vibrating knife edge is scanned through a Gaussian laser beam and a large area diameter photodiode is placed as close as possible to the knife edge, in order to pick up all the light. An appropriate bandpass filter is then employed to detect only the light time-modulated by the knife edge. Shown in Figures 2a-2e are plots generated for the first through fifth harmonics. Phase of the current is shown only for the first and second harmonic because of instrumental limitations.

It is clear that successively higher derivatives of the Gaussian beam shape are generated (note that negative values are necessarily displayed as positive, with indication of phase reversal in the case of the first and second harmonic only).

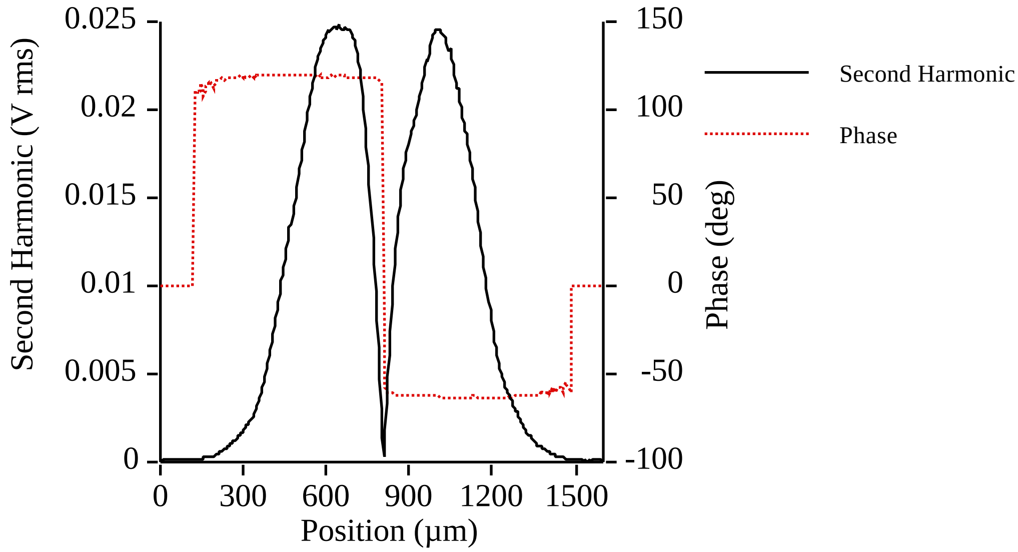
Second Harmonic (V rms)
Phase (deg)
Position (µm)
Second Harmonic
Phase
0.025
0.02
0.015
0.01
0.005
0
150
100
50
0
-50
-100
0
300
600
900
1200
1500

(b)

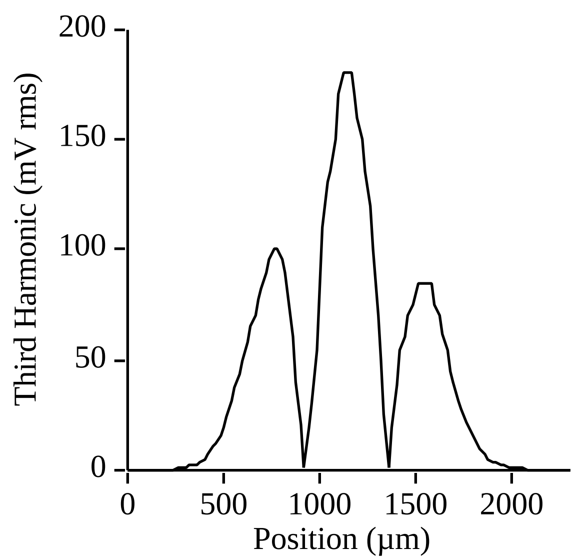
Third Harmonic (mV rms)
Position (µm)
200
150
100
50
0
0
500
1000
1500
2000

(c)

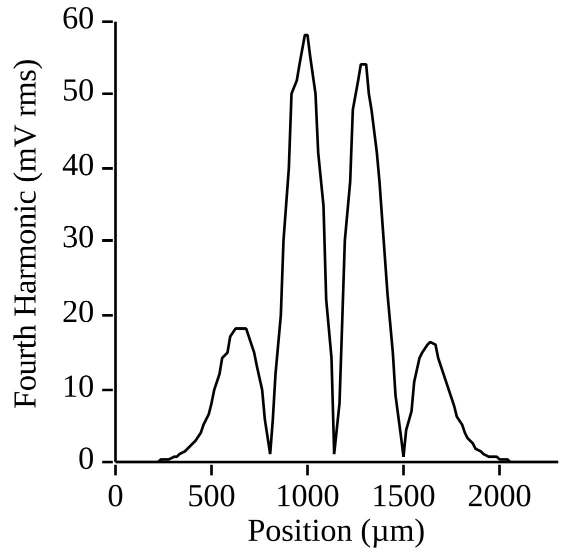

(d)

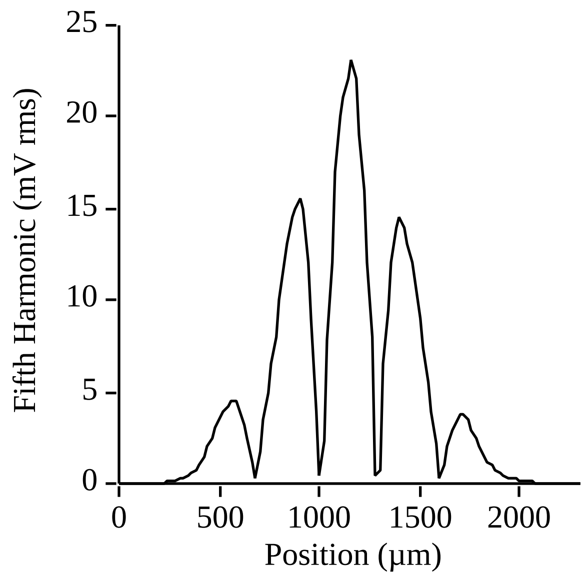

(e)

Fig. 2. Gaussian traced out by signal at a) ω, b) 2ω, c) 3ω, d) 4ω, e) 5ω

Coherent Operation

The case of coherent operation is similar to incoherent operation except that a pinhole detector is assumed to be placed on-axis in the far field of the transmitted radiation (or, alternatively in the focal plane of an infinitely large collecting lens). We then have, from (11) and (12)

$$i(t) \quad \left| \int_{-\infty}^{\infty} \int_{x(t)}^{\infty} E_i(x,y)dxdy \right|^2. \qquad (29)$$

After expanding this in a Taylor series about x_o, similar to the procedure for eq. (26), but this time only up to the first order for simplicity, it can be shown that

$$i(t) \quad i_o + a \cdot \cos(\omega t). \qquad (30)$$

In terms of the quantities

$$A_o = \int_{-\infty}^{\infty} \int_{x_o}^{\infty} E_i(x,y)dxdy \qquad (31)$$

$$A_\omega = \int_{-\infty}^{\infty} E_i(x_o,y)dy \qquad (32)$$

we find

$$i_o = A_o A_o^* - \frac{1}{2} |A_\omega|^2 \Delta^2 - \frac{1}{4} \Delta^2 (A_o A_{2\omega}^* + A_o^* A_{2\omega}) \qquad (33)$$

$$a = -(A_o A_\omega^* + A_o^* A_\omega)\Delta = -2\mathrm{Re}\{A_o A_\omega^*\}\Delta. \qquad (34)$$

4. Phase Detection

The parameters A_0 and A_ω, necessary to express the DC and first harmonic components of the modulated light are given by eqs (31) and (32). If the phases of A_o and A_ω above are indicated by φ_o and φ_ω, then

$$A_o = |A_o| \exp(j\varphi_o) \qquad (35)$$

$$A_\omega = |A_\omega| \exp(j\varphi_\omega). \qquad (36)$$

With the first time harmonic component of the current from the coherent operation given by eq. (34), we then have

$$a = -2\,|A_o A_\omega| \cos(\varphi_\omega - \varphi_o)\Delta. \qquad (37)$$

Thus the coherent mode offers the possibility of measuring the phase between the ω-labeled light [i.e the light in the vibration zone of the knife edge, eq. (32)] and the integrated surrounding field as defined by eq. (31). Note that for maximum usefulness, the reference phase, φ_o, should be $\pi/2$ in eq. (37) so that cos $(\varphi_\omega - \varphi_o)$ = sin (φ_ω). For small φ_ω (as is the case for many phase objects of interest) we then have sin (φ_ω) φ_ω and linear operation results.

In what follows we shall examine (34) in more detail by applying it to the field behind a lens.

<u>Lens as Phase Object</u>

If a lens is scanned through the vibrating knife edge, assumed to be in the same plane, the effective field E_i to be scanned can be represented by

$$E_i(x) = \exp(-x^2/w_o^2) \cdot \exp\left[\frac{-jk(x-x_s)^2}{2F}\right] \qquad (38)$$

where we will consider one-dimensional operation and ignore y dependence. The first term represents the gaussian illuminating beam with w_o being the beam waist. The second term results from scanning the lens towards the knife edge, where x_s is the distance scanned and F is the focal length of the lens. Assuming $x_o = 0$, we then find from (31)

$$A_o = \int_0^\infty \exp(-x^2/w_o^2)\cdot\exp\left[\frac{-jk(x-x_s)^2}{2F}\right]dx. \tag{39}$$

Similarly we find from (32), with $x_o = 0$

$$A_\omega = \exp\left[\frac{-jk(x_s)^2}{2F}\right] \tag{40}$$

Hence

$$A_oA_\omega^* = \int_0^\infty \exp(-x^2/w_o^2)\cdot\exp\left[\frac{-jkx^2}{2F} + \frac{jkxx_s}{F}\right]dx \tag{41}$$

and with (34), the amplitude 'a' of the first harmonic becomes

$$a \quad \mathrm{Re}\{A_oA_\omega^*\} \quad \int_0^\infty \exp(-u^2)\cdot\cos\left[\frac{-kw_o^2u^2}{2F} + \frac{kw_o^2uv}{F}\right]du \tag{42}$$

where $u = x/w_o$ and $v = x_s/w_o$.

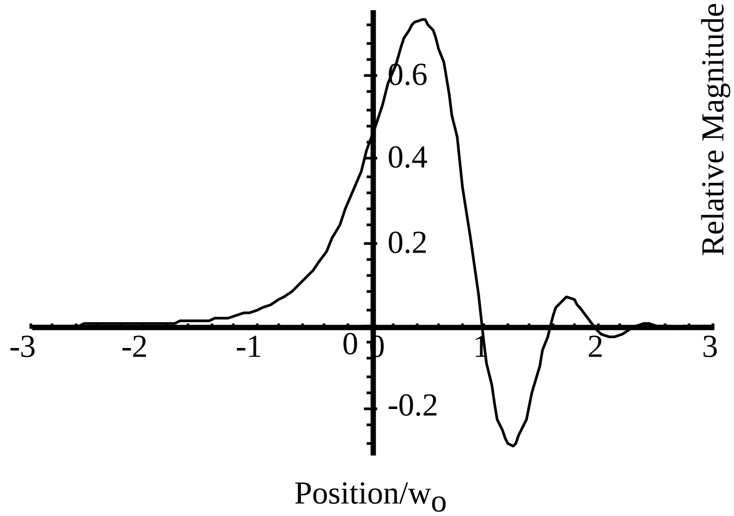

Fig. 3. Graph of expression (42); the first harmonic with 300-mm lens.

For F = 300 mm and F = 2500 mm, eq. (42) is graphed using *Maple V*, as shown in Figs. 3 and 4. Note that for the 300 mm lens the change in phase of the integrated surrounding field when scanned, produces some complex interference effects on the right hand side of the curve. Also the peak is shifted off-center. In Fig. 4 which refers to the weaker 2500 mm lens, the interference effects between A_ω and A_o are much less pronounced, and also the off-center shift is much less.

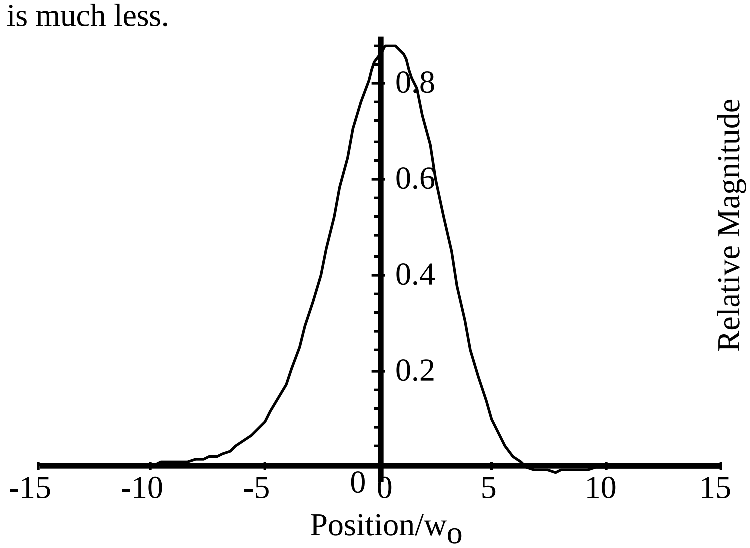

Fig. 4. Graph of expression (42); the first harmonic with a 2500-mm lens

An experimental setup to check eq. (42) is depicted in Figure 5. The phase object is 2-3 mm away from the knife edge (ideally they are in the same plane). The radiation incident upon the phase object is the light modulated by the knife edge plus the reference or background light not modulated by the knife edge.

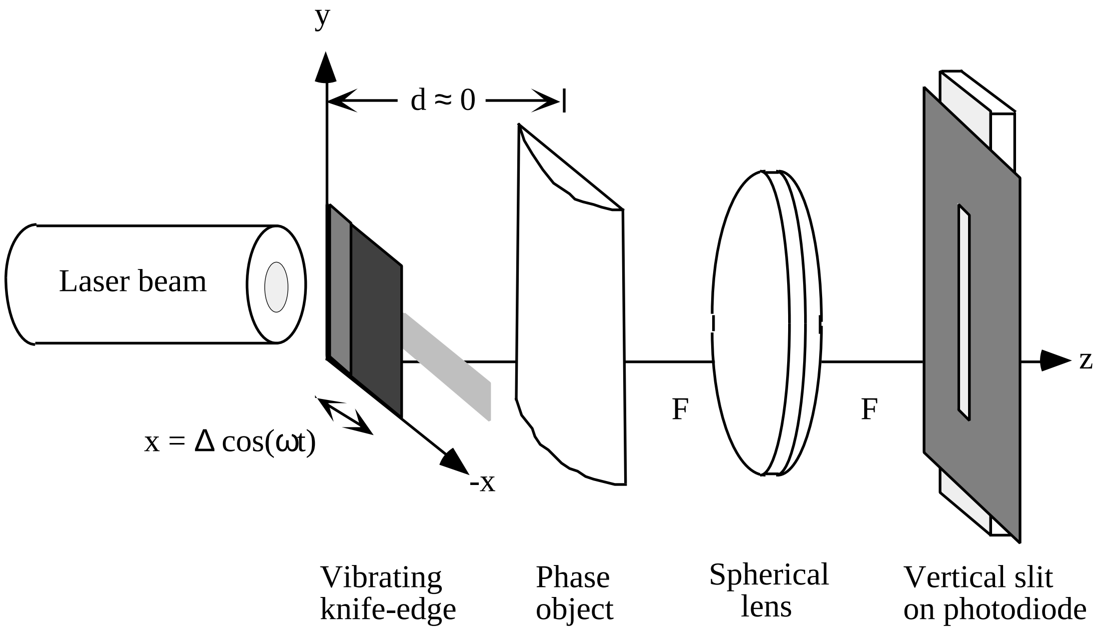

Fig. 5 Experimental setup for the scanning lens as a phase object.

A 220 mm spherical lens is used to collect the light containing phase information passing the phase object, and focus it onto a 0.1 mm vertical slit. The focused spot has a radius of about 114 μm. Figs. 6 and 7 show experimental results for the 300 mm and the 2500 mm lens respectively. Because of difficulties in visually centering the slit, the center of the lens in the 300 mm case is not well known. It can be seen that the shapes of the curves in Fig. 6 and 7 are strikingly similar to those in Figs 3 and 4 if in the latter, negative peaks are flipped positive.

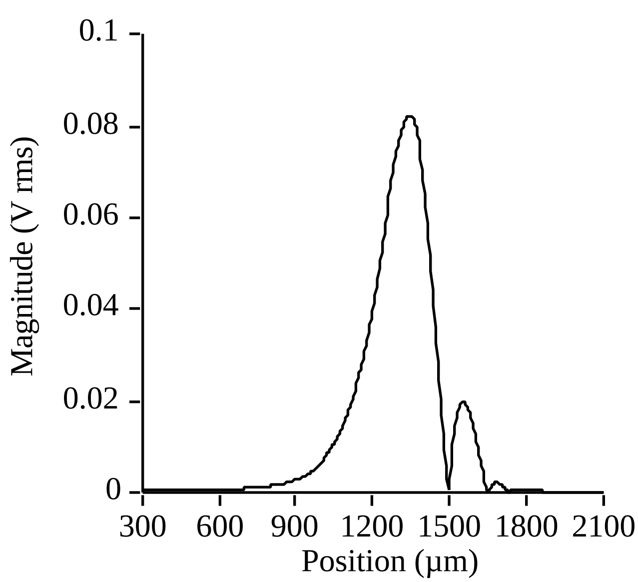

Fig. 6. First-harmonic scan of the 300-mm lens.

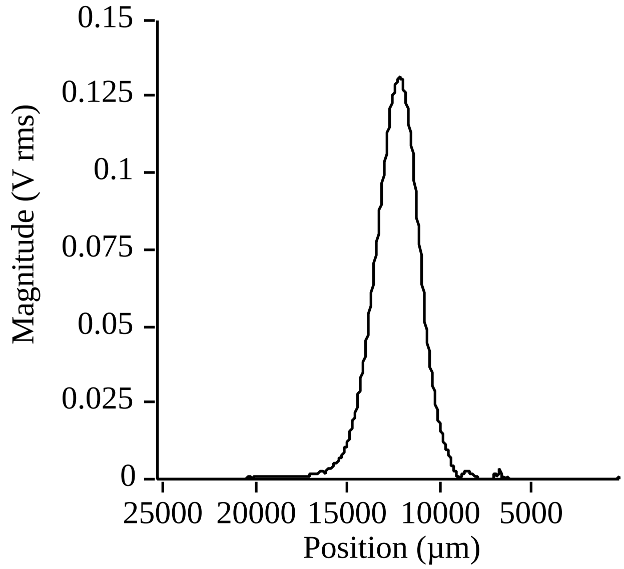

Fig. 7. First-harmonic scan of the 2500-mm lens.

5. Discussion

In the incoherent mode, some interesting edge detection features are realized by detecting higher harmonics of the current induced by the vibrating edge.These are similar to the ones utilized in wobbling-beam microscopy [6], which, as our scheme, offers electronically variable resolution.

In the coherent mode, the relative phase of the object affects the amplitude of the detected signal. "Relative" means relative to the phase of the surrounding object not directly under the vibrating knife edge. Unless this surrounding phase averages out, the measurement of the local phase is of limited value. There do exist objects that average out the phase: a phase grating with multiple periods covered by the beam is one example. However, in general it would be advisable to have a larger and stronger part of the beam fall outside the object. In that case any reference phase contributions from the object are overridden by the stronger reference signal that derives from outside the object. Alternatively, a completely separate reference beam may be used, but then the advantages of a common-path configuration are lost.

Future research into use of the coherent mode for phase microscopy should address such problems in detail. The present investigation is only meant to present the fundamental principles and assess initial overall feasibility.

Acknowledgements

This research was supported by the Army Research Office under Grants DAAL-03-91-G-0014 and DAAL-03-92-G-0207. Simulations were performed using the computer algebra and graphing package *Maple V*, v. 3 .

References

1. A. Korpel, D. J. Mehrl, and S. Samson, "Beam profiling by vibrating knife edge: implications for near field optical microscopy," Int. Jnl. of Imaging Systems and Technology **2**, 203-208 (1990).

2. A. Korpel, S. Samson, and K. Feldbush, "Two-dimensional operation of a scanning optical microscope using a vibrating knife edge corner," Int. Jnl. of Imaging Systems and Technology **4**, 207-213 (1992).

3. A. Korpel, S. Samson, and K. Feldbush, "Progress in vibrating stylus near field microscopy," *Near Field Optics* . D. W. Pohl and D. Courjon Eds., Kluwer Academic Publishers, Netherlands, 399-406 (1993).

4. S. Samson, and A. Korpel, "Two-dimensional operation of a scanning optical microscope by vibrating knife-edge tomography," Applied Optics **34**, 285-289 (1995).

5. J. Goodman, *Introduction to Fourier Optics*, McGraw-Hill Book Co., (1968).

6. M. Storrs, and D. J. Mehrl, "Detection of spatial derivatives of images using spatiotemporal techniques," Optical Engineering **33**, 3072-3081 (1994).